ISSN: 2454-1907
DOI:https://doi.org/10.29121/ijetmr.v4.i12.2017.137

IJETMR
International Journal of Engineering Technologies and Management Research
A Knowledge Repository

INVESTIGATION OF HEAT TRANSFER OF NON-NEWTONIAN FLUID IN THE PRESENCE OF A POROUS WALL

Navneet Kumar Singh [1], Ramesh Yadav [*2]

[1] Department of Mathematics Babu Banarasi Das Northern India Institute of Technology Lucknow U.P., India

[*2] Department of Mathematics Babu Banarasi Das National Institute of Technology & Management Lucknow, U.P., India

Abstract:

This study deals the investigation of heat transfer of non-Newtonian fluid in the presence of a porous bounding wall. Perturbation method is applied for the solution of non-linear differential equation. The main focus of this paper is to investigate the effects of parameters such as Reynolds number Re, Prandtl number Pr, permeability parameter K and n in the velocity of fluid and temperature coefficient. For fulfilling the purpose Matlab software has been used. The results show that velocity of non-Newtonian increases with increase of Reynolds number Re and temperature increases with increases of Prandtl number Pr.

Keywords: *Non-Newtonian Fluid; Reynolds number; Prandtl number; Porous Media; permeability parameter.*

Cite This Article: Navneet Kumar Singh, and Ramesh Yadav. (2017). "INVESTIGATION OF HEAT TRANSFER OF NON-NEWTONIAN FLUID IN THE PRESENCE OF A POROUS WALL." *International Journal of Engineering Technologies and Management Research,* 4(12), 74-92. DOI: https://doi.org/10.29121/ijetmr.v4.i12.2017.137.

1. Introduction

The non-Newtonian fluid flow through a porous medium produced by temperature differences is one of the most considerable and contemporary subjects and found the great applications, in geothermic, geophysics, chemicals, cosmetics, pharmaceuticals and industrial technology. The practical interest in convective heat transfer in porous medium is expanded rapidly, due to the wide range of applications in engineering fields. Rivlin (1955) has studied plane strain of a net formed by inextensible cords. Christopher and Middleman (1965) have studied power-law flow through a packed tube. Blottner (1970) has studied finite-difference methods of solution of the boundary-layer equations.

Chamkha (1977) has studied similarity solution for thermal boundary layer on a stretched surface of a non-Newtonian fluid. Dharmadhikari and Kale (1985) have studied flow of non-Newtonian fluids through porous media. Chen and Chen (1988) have studied free convection of non-Newtonian fluids along a vertical plate embedded in a porous medium. Wang Chaoyang and Tu Chuanjing (1989) have studied boundary-layer flow and heat transfer of non-Newtonian fluids in

ISSN: 2454-1907
DOI: 10.5281/zenodo.1140081

porous media. Hooper et al. (1993) have studied mixed convection from a vertical plate in porous media with surface injection or suction. Choi (1995) has studied enhancing thermal conductivity of fluids with nanoparticles in developments and applications of non-Newtonian flows. Das et al. (1996) have studied radiation effects on flow past an impulsively started infinite isothermal plate. Yih (1998) has studied Coupled heat and mass transfer in mixed convection over a wedge with variable wall temperature and concentration in porous media: The entire regime. Magyari et al. (1999) have studied heat and mass transfer in the boundary layers on an exponentially stretching continuous surface.

Yih (2001) has studied radiation effects on mixed convection over an isothermal wedge in the porous media: The entire regime. Wang (2002) has studied flow due to a stretching boundary with partial slip: an exact solution of the navier–stokes equations. Ingham et al. (2004) have studied Emerging Technologies and Techniques in Porous Media. Kluwer, Dordrecht, Plate with time dependant temperature and concentration. Aboeldahab and A. G. El-Din (2005) have studied thermal radiation effects on MHD flow past a semi-infinite inclined plate in the presence of mass diffusion. Mahmoud and Mahmoud (2006) have studied Analytical solutions of hydro magnetic boundary layer flow of a non-Newtonian power law fluid past a continuously moving surface. Marinca and Herisanu (2008) have studied optimal homotopy asymptotic method with application to thin film flow. Cheng (2009) has studied combined heat and mass transfer in natural convection flow from a vertical wavy surface in a power-law fluid saturated porous medium with thermal and mass stratification. Suratiand and Timol (2010) have studied numerical study of forced convection wedge flow of some non-Newtonian fluids. Bhattacharyya et al. (2011) have studied steady boundary layer slip flow and heat transfer over a flat porous plate embedded in a porous media. Ganji et al. (2011) have studied analytical heat transfer investigation of non-Newtonian fluid flow in an axisymmetric channel with a porous wall. Moorthy and Senthilvadivu (2012) have studied effect of variable viscosity on free flow of non-Newtonian power law fluids along a vertical surface with thermal stratification. Shyam et al. (2013) have studied natural convection heat transfer from two vertically aligned circular cylinders in power-law fluids. M. R. Hajmohammadi and Nourazar (2014) have studied conjugate forced convection heat transfer from a heated flat plate of finite thickness and temperature-dependent thermal conductivity. Sharma and Ishak (2014) have studied second order slip flow of cu-water nano fluid over a stretching sheet with heat transfer. Hayat et al. (2015) have studied flow of power-law nanofluid over a stretching surface with Newtonian heating. Ram Reddy et al. (2015) have studied similarity solution for free convection flow of a Micropolar fluid under convective boundary condition via Lie scaling group transformations.

In this study perturbation Technique is applied to find the approximate solution of nonlinear differential equation for non-Newtonian fluid flow in axisymmetric channel with a porous wall for turbine cooling applications. The results are given for the velocity of non-Newtonian fluid and temperature for various values of Reynolds number Re, Prandtl number Pr, permeability parameter K and parameter n.

2. Mathematical Formulation

In this paper we study the simultaneous development of fluid flow and heat transfer of non-Newtonian fluid flow is investigated, it is the applicable on the turbine disc for the cooling

ISSN: 2454-1907
DOI: 10.5281/zenodo.1140081

purposes. The problem is shown schematically in Fig. 1. In this Figure y-axis is perpendicular to the heated disc surface, which is shown the x-axis. The porous wall is parallel to heated disc axis. The perforated disc of the channel is located at y = +L. The non-Newtonian fluid is injected from the other porous wall uniformly in order to cool the heated wall that coincides with the x-axis.

Here we observed in Figure 1 the cooling problem of the disk can be considered as a inactivity point flow with injection. For a steady, axisymmetric non-Newtonian fluid flow for the following equations in the cylindrical coordinates.

The equation of continuity is

$$\frac{\partial(r\,U_r)}{\partial r}+\frac{\partial(r\,U_z)}{\partial z}=0, \tag{1}$$

Momentum equation is

$$U_r\frac{\partial(U_r)}{\partial r}+U_z\frac{\partial(U_r)}{\partial z}=-\frac{1}{\rho}\frac{\partial P}{\partial r}+\frac{1}{\rho}\left\{\frac{\partial\tau_{rr}}{\partial r}+\frac{1}{r}(\tau_{rr}-\tau_{\theta\theta})+\frac{\partial\tau_{rz}}{\partial z}\right\}, \tag{2}$$

$$U_r\frac{\partial(U_z)}{\partial r}+U_z\frac{\partial(U_z)}{\partial z}=-\frac{1}{\rho}\frac{\partial P}{\partial z}+\frac{1}{\rho}\left\{\frac{\partial\tau_{zr}}{\partial r}+\frac{1}{r}\tau_{rz}+\frac{\partial\tau_{zz}}{\partial z}\right\} \tag{3}$$

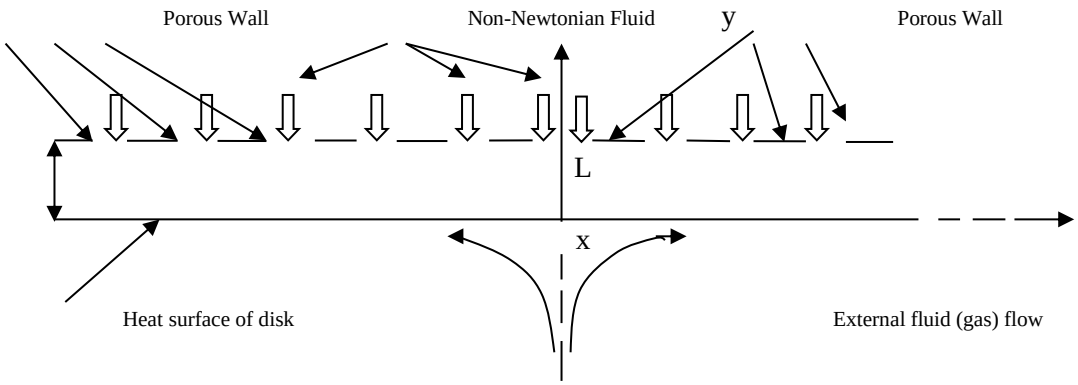

Figure 1: Schematic diagram of the formulation problem

Where τ_rr,τ_rz,τ_zr,τ_zz are the components of the stress matrix. U_r ,U_z are the velocity of fluid in the r and z directions; ρ,P are the density, Pressure of the fluids. The boundary conditions are

U_r=U_z=0 for z=0, (4)

U_r=0,U_z=-V for z=L, (5)

Here V is the injection velocity: For particular class of viscoelastic and viscoinelastic fluids Rivlin [1] showed that if the stress components τ_ij at a point x_k (k=1,2,3) and time t are

ISSN: 2454-1907
DOI: 10.5281/zenodo.1140081

considered to be polynomials in the velocity components (δv_m)/(δx_n) (m,n=1,2,3) and the acceleration components (δa_m)/(δx_n) (m,n=1,2,3), and if in addition the medium is assumed to be isotropic the stress matrix can be expressed in the form

$$\|\tau\|=\varphi_0 I+\varphi_1 A+\varphi_2 B+\varphi_3 A^2+\cdots \quad (6)$$

Here φ_k (k=0,1,2,3) is polynomials in the invariants of A,B,A^2. This study is restricted to second order fluids for which φ_k (k=0,1,2,3) are constant and φ_k (k=4,5,…) are zero, and I is the unit matrices, A and B are symmetric kinematic matrixes defined by:

$$A=\left\|\frac{\delta v_i}{\delta x_j}+\frac{\delta v_j}{\delta x_i}\right\|,\ B=\left\|\frac{\delta a_i}{\delta x_j}+\frac{\delta a_j}{\delta x_i}+2\frac{\delta v_m}{\delta x_j}\frac{\delta v_m}{\delta x_i}\right\|, \quad (7)$$

The stress components are

$$\tau_{rr}=\varphi_1 A_{rr}+\varphi_2 A_{rr}^2+\varphi_3 B_{rr}, \quad (8)$$

$$\tau_{zz}=\varphi_1 A_{zz}+\varphi_2 A_{zz}^2+\varphi_3 B_{zz}, \quad (9)$$

$$\tau_{\theta\theta}=\varphi_1 A_{\theta\theta}+\varphi_2 A_{\theta\theta}^2+\varphi_3 B_{\theta\theta}, \quad (10)$$

$$\tau_{rz}=\varphi_1 A_{rz}+\varphi_2 A_{rz}^2+\varphi_3 B_{rz}. \quad (11)$$

For the solution of this problem depicted in the figure 1 in the case of axially symmetric flow it is convenient to define a stream function so that the continuity equation is satisfied:

$$\psi=Vr^2\ f(\lambda), \quad (12)$$

Where λ=z/L and the velocity components can be derived as:

$$U_r=V_r/L\ f^{'}(\lambda)\ \&\ U_z=-2Vf(\lambda). \quad (13)$$

Using equation (12) and (13), in equation (2) and (3) and then pressure term eliminated, we get the differential equation

$$f^{IV}+2Re\ ff^{'''}-K_1 Re(4f^{''}f^{'''}+2f^{'}f^{IV})-K_2 R(4f^{''}f^{'''}+2f^{'}f^{IV}+2ff^{V})=0, \quad (14)$$

Where K_1=φ_2/(ρL^2),K_2=φ_3/(ρL^2) is injection Reynolds number, For K_2=0, the equation turned as

$$f^{IV}+2Re\ ff^{'''}-KRe(4f^{''}f^{'''}+2f^{'}f^{IV})=0, \quad (15)$$

Where K_1=K, The boundary conditions are:

$$f(0)=\ f^{'}(0)=f^{'}(1)=0\ \&\ f(1)=1. \quad (16)$$

The energy equation for this problem with viscous dissipation in non-Newtonian form is given by

ISSN: 2454-1907
DOI: 10.5281/zenodo.1140081

$$\rho C\left(U_r\frac{\partial T}{\partial r}+U_z\frac{\partial T}{\partial z}\right)=\bar{k}\,\nabla^2 T+\phi, \tag{17}$$

$$\phi=\tau_{rr}\frac{\partial U_r}{\partial r}+\tau_{\theta\theta}\frac{U_r}{r}+\tau_{zz}\frac{\partial U_z}{\partial z}+\tau_{rz}\left(\frac{\partial U_r}{\partial z}+\frac{\partial U_z}{\partial r}\right), \tag{18}$$

Where U_r,U_z are the velocity components in the r and z directions and V is the injection velocity: ρ,P,T,C,k¯ are the density, pressure, temperature, specific heat and heat conduction coefficient of the fluid, respectively, ϕ is the dissipation function. Assuming the blade wall (z=0) temperature distribution be

$$T_w=T_0+\sum_{n=0}^{\infty}C_n(r/L)^n \tag{19}$$

And assuming the fluid temperature to have the form of [1]

$$T=T_0+\sum_{n=0}^{\infty}C_n\left(\frac{r}{L}\right)^n q_n(\lambda) \tag{20}$$

Where T_0 is the temperature of the incoming coolant (z = L) and neglecting dissipation effect the following equations and boundary conditions are obtained:

q_n^''-RePr(n f^' q_n-2fq_(n)^') for (n = 0,1,2,3,4), (21)

q_n (0) =1, q_n (1) =0. (22)

The above differential equation (15) and (21) solved by perturbation technique, given bellow.

3. Method of Solution

In this paper we have applied the perturbation technique for the solution of non-linear differential equation with suitable boundary conditions, which is given above. We take the series

$$f(\lambda)=f_0(\lambda)+Ref_1(\lambda)+Re^2f_2(\lambda)+\cdots \quad =\sum_{m=0}^{\infty}Re^m\,f_m(\lambda) \tag{23}$$

$$q_n(\lambda)=q_{n0}(\lambda)+Req_{n1}(\lambda)+Re^2q_{n2}(\lambda)+\cdots \quad =\sum_{m=0}^{\infty}Re^m q_{nm}(\lambda) \tag{24}$$

Putting these values of equation (23) in equation (15), we get

$$\{f_0^{IV}(\lambda)+Ref_1^{IV}(\lambda)+Re^2f_2^{IV}(\lambda)+\cdots\}+2Re\,\{f_0(\lambda)+Ref_1(\lambda)+Re^2f_2(\lambda)+\cdots\}\{f_0'''(\lambda)+Ref_1'''(\lambda)+Re^2f_2'''(\lambda)+\cdots\}-KRe[4\{f_0''(\lambda)+Ref_1''(\lambda)+Re^2f_2''(\lambda)+\cdots\}\{f_0'''(\lambda)+Ref_1'''(\lambda)+Re^2f_2'''(\lambda)+\cdots\}+2\{f_0'(\lambda)+Ref_1'(\lambda)+Re^2f_2'(\lambda)+\cdots\}\{f_0^{IV}(\lambda)+Ref_1^{IV}(\lambda)+Re^2f_2^{IV}(\lambda)+\cdots\}]=0. \tag{25}$$

Taking the coefficient of$Re^0,\ Re^1$, we get

$$f_0^{IV}(\lambda)=0, \tag{26}$$

ISSN: 2454-1907
DOI: 10.5281/zenodo.1140081

$$f_1^{IV}(\lambda) = 4Kf_0''(\lambda)f_0'''(\lambda) - 2f_0(\lambda)f_0'''(\lambda)\ . \tag{27}$$

Putting these values of equation (24) in equation (21), we get

$$\{q_{n0}''(\lambda) + Req_{n1}''(\lambda) + Re^2q_{n2}''(\lambda) + \cdots\ \} - RePr[n\ \{f_0'(\lambda) + Ref_1'(\lambda) + Re^2f_2'(\lambda) + \cdots\}\{q_{n0}(\lambda) + Req_{n1}(\lambda) + Re^2q_{n2}(\lambda) + \cdots\} - 2\{f_0(\lambda) + Ref_1(\lambda) + Re^2f_2(\lambda) + \cdots\}\{q_{n0}'(\lambda) + Req_{n1}'(\lambda) + Re^2q_{n2}'(\lambda) + \cdots\}]. \tag{28}$$

Taking the coefficient of $Re^0,\ Re^1,\ Re^2$, we get

$$q_{n0}''(\lambda) = 0, \tag{29}$$

$$q_{n1}''(\lambda) = Pr(nq_{n0}f_0' - 2f_0q_{n0}'), \tag{30}$$

$$q_{n2}''(\lambda) = Pr[n\{q_{n0}(\lambda)\ f_1'(\lambda) + q_{n1}(\lambda)f_0'(\lambda)\} - 2\{f_0(\lambda)q_{n1}'(\lambda) + f_1(\lambda)q_{n0}'(\lambda)\}]. \tag{31}$$

Now solving the above equation (26), (27), (29), (30) and (31) using the boundary condition (16) & (22)

$$f_0(\lambda) = 3\lambda^2 - 2\lambda^3, \tag{32}$$

$$f_1(\lambda) = \left(\frac{223}{70} - \frac{6}{5}K\right)\lambda^2 - \left(\frac{79}{35} - \frac{24}{5}K\right)\lambda^3 - 6K\lambda^4 + \frac{12}{5}K\lambda^5 + \frac{1}{10}\lambda^6 - \frac{1}{35}\lambda^7. \tag{33}$$

Taking the coefficient of $R^0,\ R^1,\ R^2$, we get

$$q_{n0}(\lambda) = 1 - \lambda\ , \tag{34}$$

$$q_{n1}(\lambda) = 1 - \frac{\{10+3PrRe(n-1)\}}{10}\lambda + PrRe\left\{n\ \lambda^3 - \frac{(2n-1)}{2}\lambda^4 + \frac{(3n-2)}{10}\lambda^5\right\}, \tag{35}$$

$$q_{n2}(\lambda) = 1 - (1 - 0.0257143\ Pr^2Re^2n^2 + 0.398333\ n\ Pr^2Re^2 - 0.32246034Pr^2Re^2 - 0.333381nPrRe - 0.28KnPrRe - 0.005714286KPrRe)\lambda + Pr[n(2.061905 - 0.4\ K)\lambda^3 - \{0.2K - 5.30952 + 2.09524\ n - 1.4K\ n - 0.15PrRe\ n(n-1)\}\lambda^4 + \{0.48K + 0.074286 + 0.09\ \mathrm{Pr}(n-1) + 0.6386\ n - 1.92K\ n + 0.09PrRe\ n(n-1)\}\lambda^5 + \{0.2\ n^2PrRe + 1.2\ K\ n - 0.2 - 0.06\ \mathrm{Pr}\ Re\ (11n-1) - 0.4K\}\lambda^6 + \{0.114286\ K + 0.285743PrRe(2n-1) - 0.271429\ n - 0.0714286PrRe\ n(4n-1)\}\lambda^7 + \{0.0107143PrRe(13n-2) - 0.014286 - 0.01786PrRe(25n-11) - 0.00357143\}\lambda^8 + \{0.0194444PrRe(3n-2) - 0.003574287\}]. \tag{36}$$

ISSN: 2454-1907
DOI: 10.5281/zenodo.1140081

Now putting the value of equation (32), (33), (34), (35), (36) in equation (23) and (24), we get the solution of non-linear differential equation (15) & (21)

$$f(\lambda) = 3\lambda^2 - 2\lambda^3 + Re\left[\left(\frac{223}{70} - \frac{6}{5}K\right)\lambda^2 - \left(\frac{79}{35} - \frac{24}{5}K\right)\lambda^3 - 6K\lambda^4 + \frac{12}{5}K\lambda^5 + \frac{1}{10}\lambda^6 - \frac{1}{35}\lambda^7\right], \tag{37}$$

$$q_n(\lambda) = 1 - \lambda + Re\left[1 - \frac{\{10+3PrRe(n-1)\}}{10}\lambda + PrRe\left\{n\,\lambda^3 - \frac{(2n-1)}{2}\lambda^4 + \frac{(3n-2)}{10}\lambda^5\right\}\right] +$$
$$Re^2\big[1 - (1 - 0.0257143\,Pr^2Re^2n^2 + 0.398333\,n\,Pr^2Re^2 - 0.32246034Pr^2Re^2 -$$
$$0.333381nPrRe - 0.28KnPrRe - 0.005714286KPrRe)\lambda + Pr[n(2.061905 - 0.4\,K)\lambda^3 -$$
$$\{0.2K - 5.30952 + 2.09524\,n - 1.4K\,n - 0.15PrRe\,n(n-1)\}\lambda^4 + \{0.48K + 0.074286 +$$
$$0.09\,\mathrm{Pr}(n-1) + 0.6386\,n - 1.92K\,n + 0.09PrRe\,n(n-1)\}\lambda^5 + \{0.2\,n^2PrRe + 1.2\,K\,n -$$
$$0.2 - 0.06\,\mathrm{Pr}\,Re\,(11n-1) - 0.4K\}\lambda^6 + \{0.114286\,K + 0.285743PrRe(2n-1) -$$
$$0.271429\,n - 0.0714286PrRe\,n(4n-1)\}\lambda^7 + \{0.0107143PrRe(13n-2) - 0.014286 -$$
$$0.01786PrRe(25n-11) - 0.00357143\}\lambda^8 +$$
$$\{0.0194444PrRe(3n-2) - 0.003574287\}]\big] + \cdots \tag{38}$$

The Graphs have been plotted with described set of parameters and discussed in detail in the next section.

4. Results and Discussion

The objective of the present study is to find out the solution of heat transfer of non-Newtonian fluid in the presence of a porous bounding wall, for the purpose we have used the perturbation technique. In this paper the graph of non-Newtonian fluid velocity and Temperature coefficient against distance have been plotted using constant Reynolds number, Prandtl number and other parameter. Fig 2 represents the graph between dimensionless variable λ and velocity of non-Newtonian fluid f(λ): From this figure increase of dimensionless variable λ velocity of fluid increases slowly in the range($0 \le \lambda \le 1.4$). It is seen that increase of Reynolds number Re velocity of fluid increases sharply. Fig 3 represents the graph between dimensionless variable λ and fluid velocity of non-Newtonian fluid f(λ): From this increase of dimensionless variable λ velocity of fluid increases slowly in the range ($0 \le \lambda \le 1.5$) and sharply increases in the range ($1.5 \le \lambda \le 2.5$). It is seen that increase of Reynolds number Re velocity of fluid increases sharply.

Fig 4 is the graph between dimensionless variable λ and velocity of non-Newtonian fluid f(λ), increase of dimensionless variable λ velocity of non-Newtonian fluid f(λ) increases in the range ($0 \le \lambda \le 1$) at constant Reynolds number Re = 3; It is seen that increase of permeability parameter K velocity of fluid increases. Fig 5 is the same graph as fig 4 at different Reynolds number Re =

ISSN: 2454-1907
DOI: 10.5281/zenodo.1140081

9.2 and the effect of permeability parameter K is same as in the Fig 4. Whereas in from Fig 6, it is the reciprocal effect of permeability parameter K for negative Reynolds number Re = - 13.88. Fig 7 is graph between dimensionless variable λ and velocity of fluid f(λ), increase of dimensionless variable λ velocity of non-Newtonian fluid f(λ) increases slowly in the (0≤λ≤1.5) then increases sharply in the range (1.5≤λ≤2.5); it is seen that increase of permeability parameter K velocity of fluid increases sharply.

Fig 8a & 8b is graph between dimensionless variable λ and radial velocity of non-Newtonian fluid f'(λ) at constant Reynolds number Re = 2, increase of dimensionless variable λ in the range (0≤λ≤1) radial velocity of fluid increases sharply then decreases sharply. This curve is like as half sine nature; it is seen that increase of permeability parameter K the sharpness of radial velocity of fluid increases. Fig 9a represents the graph between dimensionless variable λ and radial velocity of fluid f^' (λ) at constant parameter K = 0.5 in the range(0≤λ≤1), increase of dimensionless variable λ radial velocity of fluid f^' (λ) slowly increases then decreases, it is flat type curve; it is seen that the increase of Reynolds number Re radial velocity of fluid f^' (λ) increases sharply then decreases sharply, it is peaked type of curve. Fig 9b represents the graph between dimensionless variable λ and radial velocity of fluid f^' (λ) at constant variable K = 0.5 in the range (0≤λ≤2.5), increase of dimensionless variable λ radial velocity of fluid f^' (λ) slowly increases then decreases slowly in the range (0≤λ≤1.5), and increases sharply in the range (1.5≤λ≤2.5); it is seen that the increase of Reynolds number Re radial velocity of fluid f^' (λ) increases sharply then decreases sharply.

Fig 10 represents the graph between dimensionless variable λ and temperature coefficient of fluid qn(λ) at constant variable Re = 0.5, Pr = 3.0, n = 2.0 in the range(0≤λ≤1), increase of dimensionless variable λ the temperature coefficient of fluid qn(λ) decreases slowly then increases sharply: it is seen that the increase of permeability parameter K temperature coefficient of fluid qn(λ) increases. Fig 11 represents the graph between dimensionless variable λ and temperature coefficient of fluid qn(λ) at constant variable k = 0.5, Pr = 3.0, n = 2.0 in the range(0≤λ≤1), increase of dimensionless variable λ the temperature coefficient of fluid qn(λ) decreases slowly then increases sharply: it is seen that the increase of Reynolds number Re temperature coefficient of fluid qn(λ) increases sharply.

Fig 12 represents the graph between dimensionless variable λ and temperature coefficient of fluid qn(λ) at constant variable k = 0.5, Re = 1.0, n = 2.0 in the range(0≤λ≤1), increase of dimensionless variable λ the temperature coefficient of fluid qn(λ) decreases slowly then increases sharply: it is seen that the increase of Prandtl number Pr temperature coefficient of fluid qn(λ) increases more sharply as compared to other results. Fig 13 represents the graph between dimensionless variable λ and temperature coefficient of fluid qn(λ) at constant variable k = 0.5, Pr = 3.0, Re = 1.0 in the range(0≤λ≤1), increase of dimensionless variable λ the temperature coefficient of fluid qn(λ) decreases slowly then increases sharply: it is seen that the increase of Parameter n temperature coefficient of fluid qn(λ) decreases then increases sharply.

Fig 14a represents the graph between dimensionless variable λ and temperature coefficient of fluid qn(λ) at constant variable k = 0.5, Pr = 3.0, Re = 0.5 in the range(0≤λ≤1), increase of dimensionless variable λ the temperature coefficient of fluid qn(λ) decreases slowly then

ISSN: 2454-1907
DOI: 10.5281/zenodo.1140081

increases sharply: it is seen that the increase of Parameter n temperature coefficient of fluid qn(λ) increases sharply. The reciprocal effect has shown in the Fig. 14b. It is seen that increase of parameter n temperature coefficient of fluid qn(λ) is decreases sharply at constant parameter k = 0.5, Pr = 3.0, Re = 2.0 in the range(0≤λ≤1).

Fig 15a represents the graph between dimensionless variable λ and temperature coefficient of fluid qn'(λ) at constant variable k = 0.01, Pr = 1.0, Re = 2.0 in the range (0≤λ≤1), increase of dimensionless variable λ the temperature coefficient of fluid qn'(λ) increases sharply: it is seen that the increase of parameter n temperature coefficient of fluid qn'(λ) increases. Fig 15b represents the graph between dimensionless variable λ and temperature coefficient of fluid qn'(λ) at constant variable K = 0.01, Pr = 3.0, Re = 2.0 in the range (0≤λ≤1), increase of dimensionless variable λ the temperature coefficient of fluid qn'(λ) increases sharply: it is been seen that the increase of Parameter n temperature coefficient of fluid qn'(λ) decreases sharply.

Fig 16 represents the graph between dimensionless variable λ and temperature coefficient of fluid qn'(λ) at constant variable k = 0.01, n = 2.0, Re = 2.0 in the range(0≤λ≤1), increase of dimensionless variable λ the temperature coefficient of fluid qn'(λ) slowly increases then slowly decreases: it is seen that the increase of Prandtl number Pr temperature coefficient of fluid qn'(λ) increases sharply then decreases sharply.

Fig 17 represents the graph between dimensionless variable λ and temperature coefficient of fluid qn'(λ) at constant variable Pr = 3.0, n = 2.0, Re = 2.0 in the range(0≤λ≤1), increase of dimensionless variable λ the temperature coefficient of fluid qn'(λ) slowly increases then sharply decreases: it is seen that the increase of variable k temperature coefficient of fluid qn'(λ) increases then decreases sharply.

Fig 18 represents the graph between dimensionless variable λ and temperature coefficient of fluid qn'(λ) at constant variable Pr = 3.0, n = 2.0, k = 0.5 in the range(0≤λ≤1), increase of dimensionless variable λ the temperature coefficient of fluid qn'(λ) slowly increases: it is seen that the increase of Reynolds number Re temperature coefficient of fluid qn'(λ) increases sharply. Fig 19 represents the graph between dimensionless variable λ and axial & radial velocity of fluid f(λ) & f'(λ) at constant variable k = 0.01, Re = 2.0 in the range(0≤λ≤1), increase of dimensionless variable λ the axial velocity of fluid f(λ)slowly increases and radial velocity of fluid f'(λ) increases sharply. Fig 20 represents the graph between dimensionless variable λ and temperature coefficient of fluid qn(λ) & qn'(λ) at constant variable Pr = 3.0, n = 2.0, k = 0.01 in the range(0≤λ≤1), increase of dimensionless variable λ the temperature coefficient of fluid qn(λ) slowly increases: and temperature coefficient of qn'(λ) increases sharply then decreases sharply.

ISSN: 2454-1907
DOI: 10.5281/zenodo.1140081

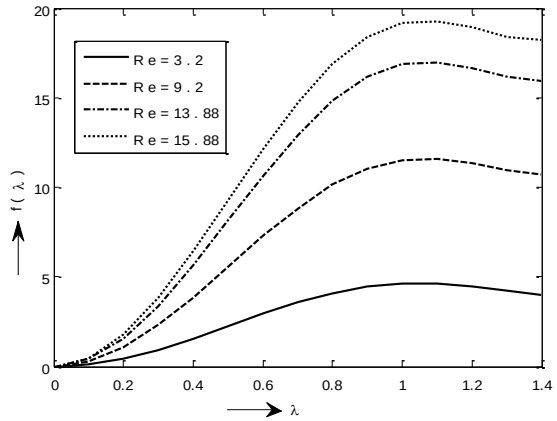

Figure 2: Graph between the dimensionless variable λ against velocity of fluid $f(\lambda)$ at constant value of K = 0.5

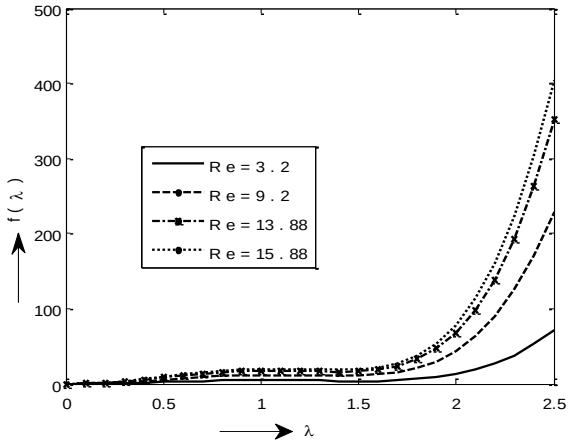

Figure 3: Graph between the dimensionless variable λ against velocity of fluid $f(\lambda)$ at constant value of K = 0.5

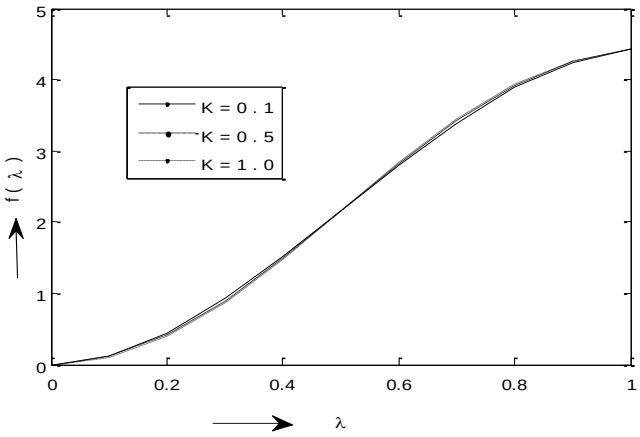

Figure 4: Graph between the dimensionless variable λ against velocity of fluid $f(\lambda)$ at constant value of Re = 3.

ISSN: 2454-1907
DOI: 10.5281/zenodo.1140081

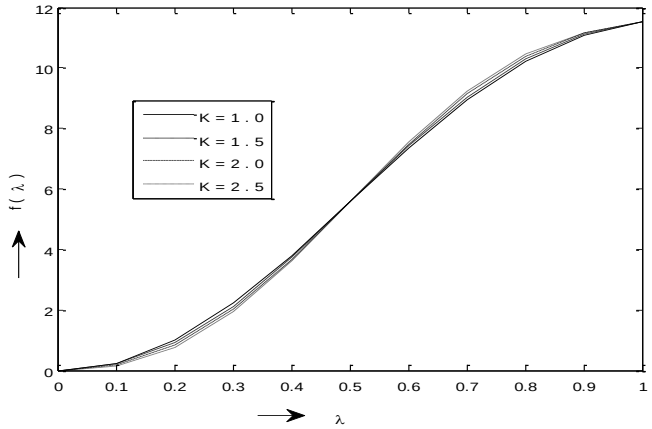

Figure 5: Graph between the dimensionless variable λ against axial velocity of fluid $f(\lambda)$ at constant value of Re = 9.2.

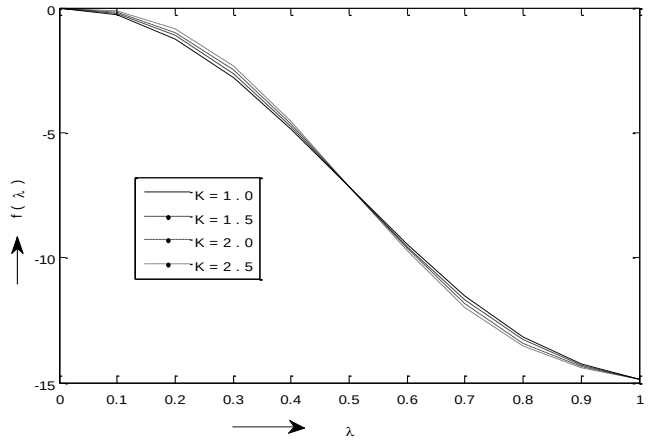

Figure 6: Graph between the dimensionless variable λ against velocity of fluid $f(\lambda)$ at constant value of Re = –13.88.

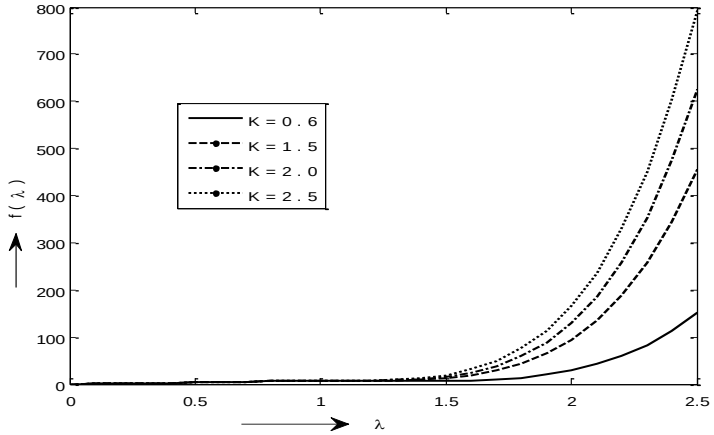

Figure 7: Graph between the dimensionless variable λ against velocity of fluid $f(\lambda)$ at constant value of Re = 5.

ISSN: 2454-1907
DOI: 10.5281/zenodo.1140081

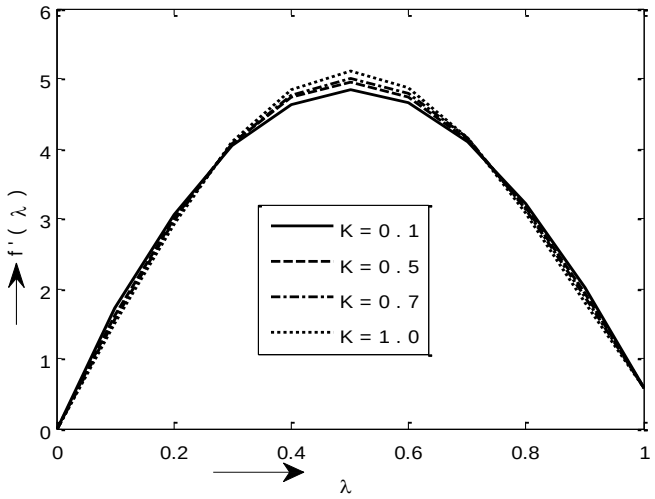

Figure 8a: Graph between the dimensionless variable λ against radial velocity of fluid $f'(\lambda)$ at constant value of Re = 2.0.

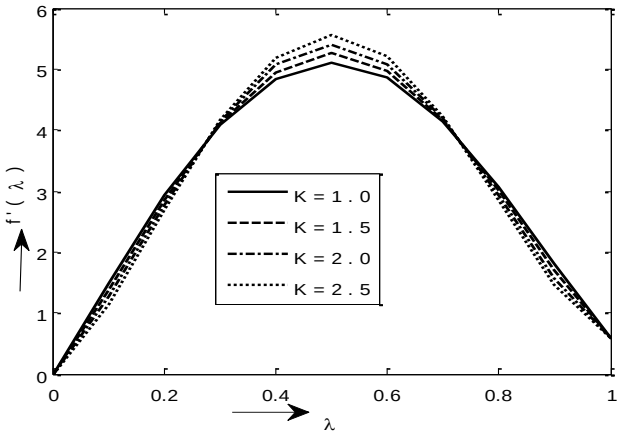

Figure 8b: Graph between the dimensionless variable λ against radial velocity of fluid $f'(\lambda)$ at constant value of Re = 2.0.

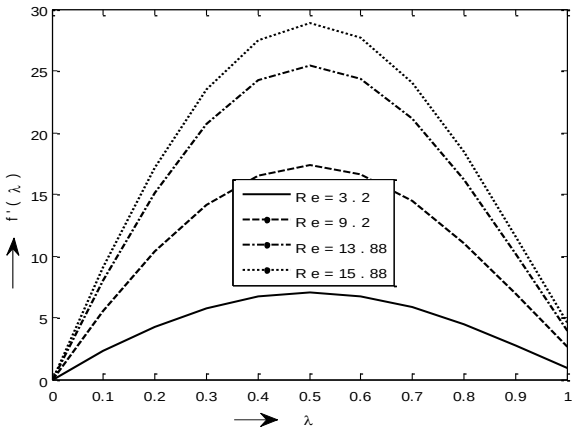

Figure 9a: Graph between the dimensionless variable λ against radial velocity of fluid $f'(\lambda)$ at constant value of K = 0.5.

ISSN: 2454-1907
DOI: 10.5281/zenodo.1140081

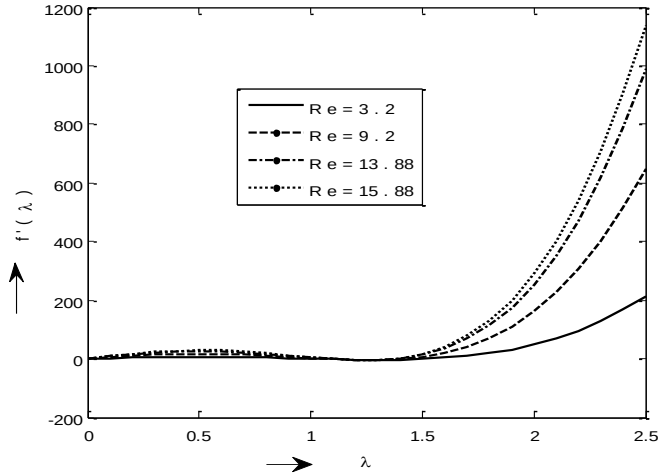

Figure 9b: Graph between the dimensionless variable λ against radial velocity of fluid $f'(\lambda)$ at constant value of K = 0.5.

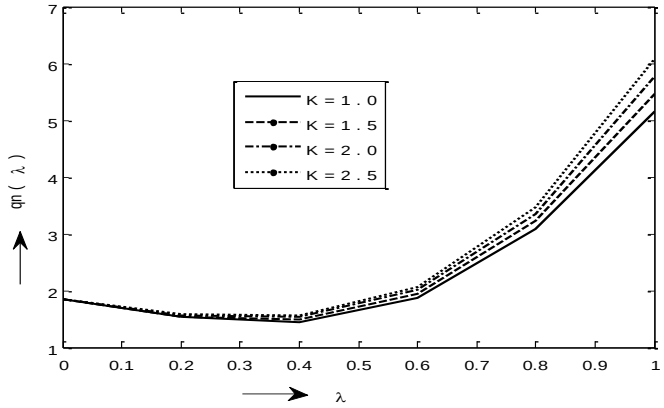

Figure 10: Graph between the dimensionless variable λ against heat transfer of fluid qn(λ) at constant value of Re = 0.5, Pr = 3, n = 2.

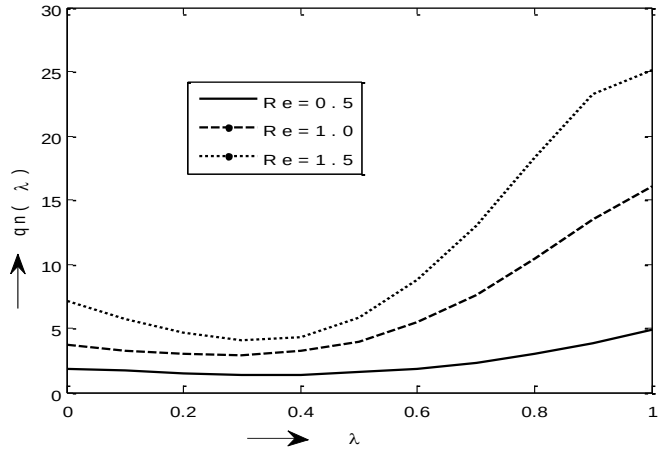

Figure 11: Graph between the dimensionless variable λ against heat transfer of fluid qn(λ) at constant value of K = 0.5, Pr = 3, n = 2.

ISSN: 2454-1907
DOI: 10.5281/zenodo.1140081

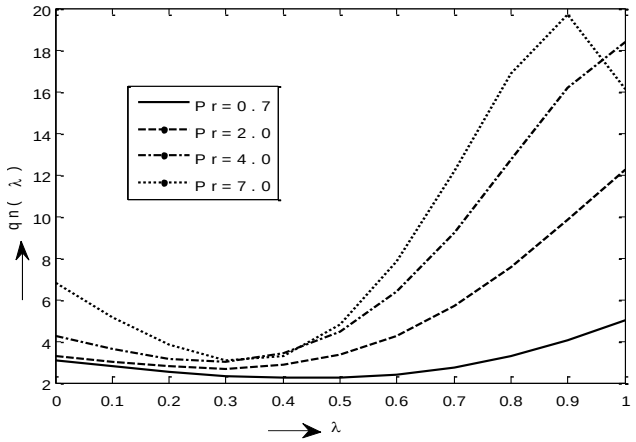

Figure 12: Graph between the dimensionless variable λ against heat transfer of fluid qn(λ) at constant value of Re = 1, K = 0.5, n = 2.

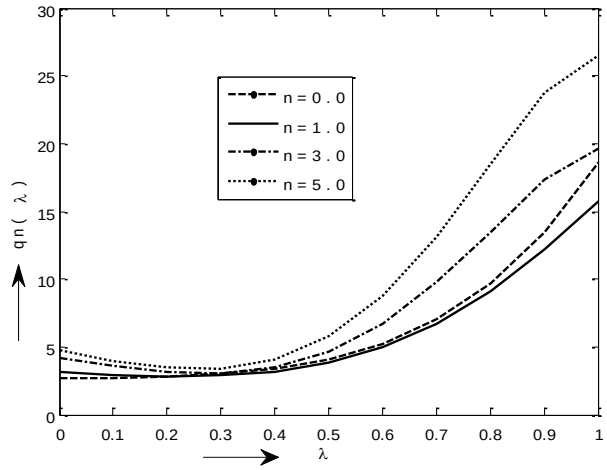

Figure 13: Graph between the dimensionless variable λ against heat transfer of fluid qn(λ) at constant value of Re = 0.5, Pr = 3, K = 0.5

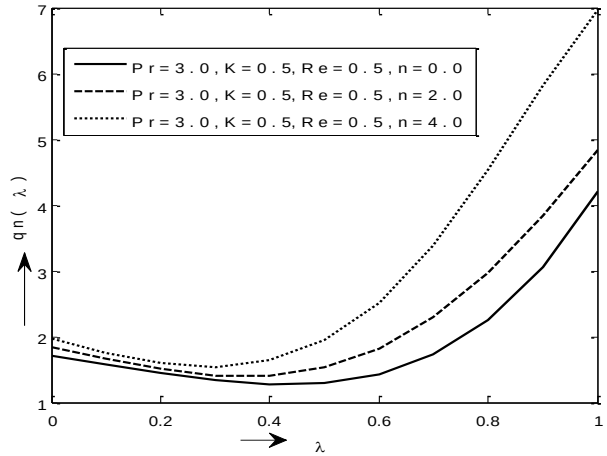

Figure 14a: Graph between the dimensionless variable λ against heat transfer of fluid qn(λ) at constant value of variable

ISSN: 2454-1907
DOI: 10.5281/zenodo.1140081

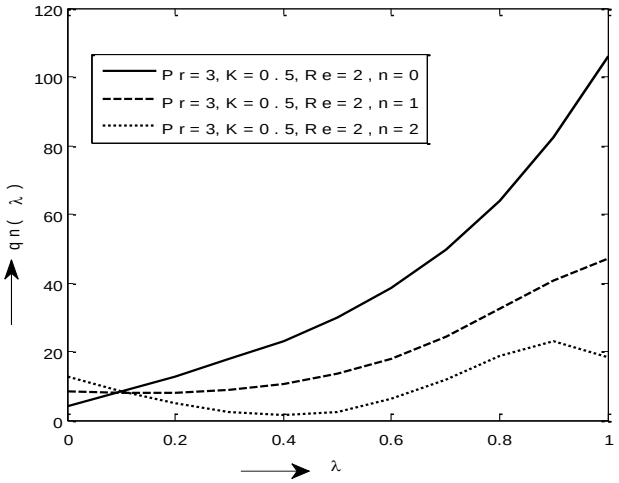

Figure 14b: Graph between the dimensionless variable λ against heat transfer of fluid qn(λ) at constant value of variable.

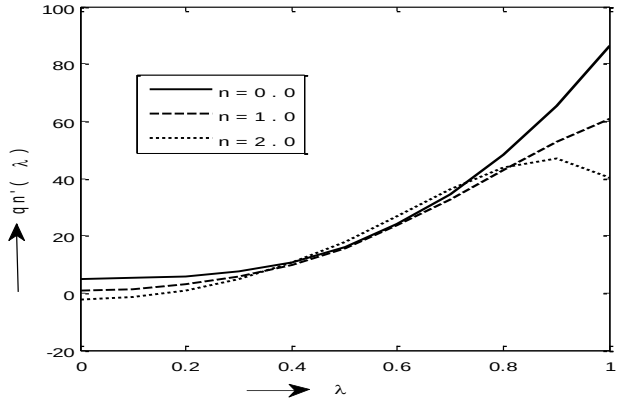

Figure 15a: Graph between the dimensionless variable λ against heat transfer of fluid qn$'$(λ) at constant variable K = 0.01, Pr = 1, Re = 2.

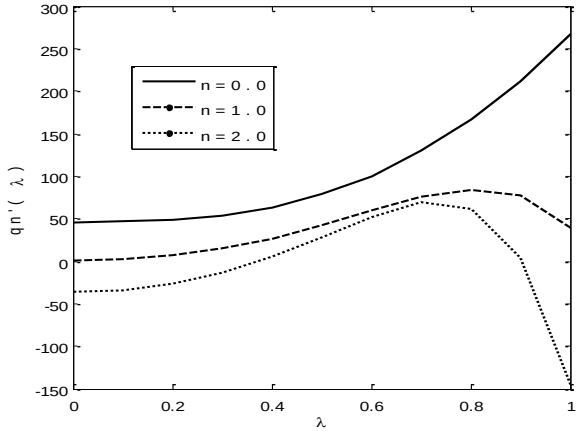

Figure 15b: Graph between the dimensionless variable λ against heat transfer of fluid qn$'$(λ) at constant variable K = 0.01, Pr = 3, Re = 2.

ISSN: 2454-1907
DOI: 10.5281/zenodo.1140081

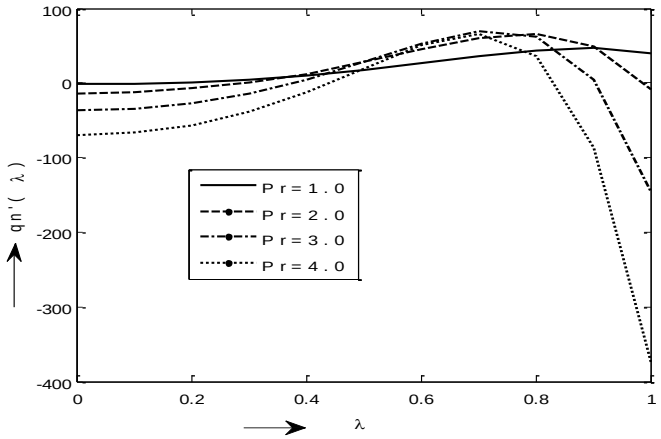

Figure 16: Graph between the dimensionless variable λ against heat transfer of fluid $qn'(\lambda)$ at constant variable K = 0.01, n = 2, Re = 2.

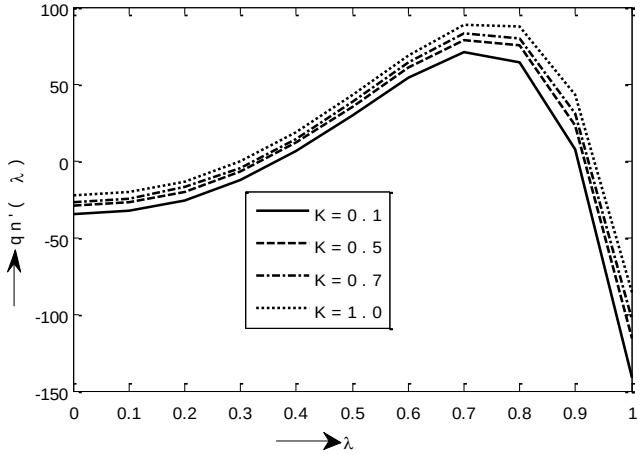

Figure 17: Graph between the dimensionless variable λ against heat transfer of fluid $qn'(\lambda)$ at constant variable n = 2, Pr = 3, Re = 2.

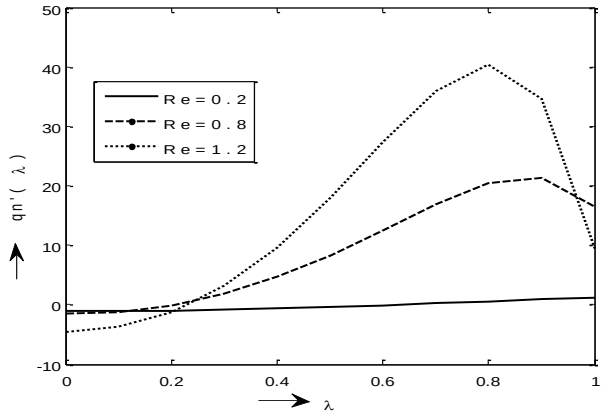

Figure 18: Graph between the dimensionless variable λ against heat transfer of fluid $qn'(\lambda)$ at constant variable K = 0.01, Pr = 3, n = 2.

ISSN: 2454-1907
DOI: 10.5281/zenodo.1140081

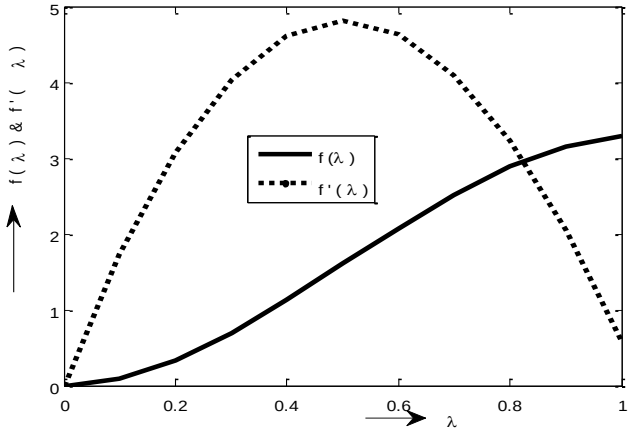

Figure 19: Graph between the dimensionless variable λ against axial and radial velocity of fluid $f(\lambda)$ & $f'(\lambda)$ at constant variable K = 0.01, Re = 2.

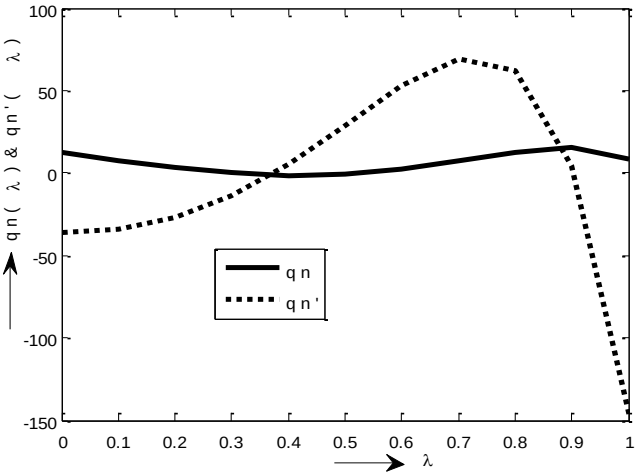

Figure 20: Graph between the dimensionless variable λ against heat transfer of fluid $qn(\lambda)$ & $qn'(\lambda)$ at constant variable K = 0.01, Pr = 3, n = 2.

5. Conclusions

In this paper the main objective is to investigate the effect of Reynolds number Re, Prandtl number Pr, permeability parameter k and parameter n. The results show that the increment in the Reynolds number has the similar effects on velocity components and heat component. It increases sharply. At higher Reynolds number the maximum velocity of fluid is shift to the solid wall where shear stress becomes larger as the Reynolds number grows. The increase of permeability parameter k velocity of fluid increases whereas the heat coefficient of fluid is also increased. Increase of Prandtl number Pr heat flow of fluid increases sharply. Increase of parameter n heat flow of fluid decreases sharply. It is investigated that Reynolds numbers sharply affect the velocity of fluid and heat flow of fluid. This study have practical applications in nuclear engineering control, plasma aerodynamics, mechanical engineering manufacturing processes, astrophysical fluid dynamics, filtration technology, geothermal energy and precipitation.

ISSN: 2454-1907
DOI: 10.5281/zenodo.1140081

References

[1] R. S. Rivlin, (1955); 'Plane strain of a net formed by inextensible cords.' Jour. of Rational Mech. Anal 4, pp. 323.
[2] R. H. Christopher and S. Middleman, (1965); 'Power-law flow through a packed tube.' I & EC Fundamentals, Vol. 4, pp. 422-426.
[3] F. G. Blottner, (1970); 'Finite-difference methods of solution of the boundary-layer equations.' AIAA Journal, Vol. 8, pp. 193-205.
[4] A. J. Chamkha, (1977); 'Similarity solution for thermal boundary layer on a stretched surface of a non-Newtonian fluid.' International Communications in Heat and Mass Transfer, vol. 24, pp. 643-652.
[5] R. V. Dharmadhikari and D.D. Kale, (19850; 'Flow of non-Newtonian fluids through porous media.' Chemical Eng. Sci., Vol. 40, pp. 527 – 529.
[6] H. T. Chen and C.K. Chen, (1988); 'Free convection of non- Newtonian fluids along a vertical plate embedded in a porous medium.' Trans. ASME, J. Heat Transfer, Vol. 110, pp. 257 – 260.
[7] Wang Chaoyang and Tu Chuanjing, (1989); 'Boundary-layer flow and heat transfer of non-Newtonian fluids in porous media.' Int. d. Heat and Fluid Flow, Vol. 10, No. 2, pp.160 – 165.
[8] W.B. Hooper, T.S. Chen and B.F., (1993); 'Armaly mixed convection from a vertical plate in porous media with surface injection or suction.' Numer. Heat Transfer, Vol. 25, pp. 317 – 329.
[9] Choi, S. U. S., (1995); 'Enhancing thermal conductivity of fluids with nanoparticles in developments and applications of non-Newtonian flows.' ASME, FED-vol. 231/MD-vol. 66, pp. 99 – 105.
[10] Das, U. N, Deka, R. K. and Soundalgekar, V. M. (1996); 'Radiation effects on flow past an impulsively started infinite isothermal plate.' Journal of Theoretical Mechanics, Vol. 1, pp. 111 – 115.
[11] K.A. Yih, (1998); 'Coupled heat and mass transfer in mixed convection over a wedge with variable wall temperature and concentration in porous media: The entire regime.' Int. Commun. Heat Mass Transfer, Vol. 25, pp. 1145 – 1158.
[12] Magyari, E., and Keller, B., (1999); 'Heat and mass transfer in the boundary layers on an exponentially stretching continuous surface.' Journal of Physics D, Vol. 32, No. 5, pp. 577 – 585.
[13] K.A. Yih, (2001); 'Radiation effects on mixed convection over an isothermal wedge in the porous media: The entire regime.' Heat Transfer Engineering, Vol. 22, pp. 26 – 32.
[14] Wang C. Y. (2002); 'Flow due to a stretching boundary with partial slip: an exact solution of the navier–stokes equations.' Acta Mechanica, Vol. 57, pp. 3745.
[15] Ingham, D. B., Bejan, A., Mamut, E. and Pop, I. (2004); 'Emerging Technologies and Techniques in Porous Media. Kluwer, Dordrecht, Plate with time dependant temperature and concentration.' International Journal of Pure and Applied Mathematics, Vol. 23, pp. 759 – 766.
[16] Aboeldahab, E. M. and El-Din, A. G., (2005); 'Thermal radiation effects on MHD flow past a semi-infinite inclined plate in the presence of mass diffusion.' Heat and Mass Transfer, Vol. 41(12), pp. 1056 – 1065.
[17] Mahmoud M. A. A., Mahmoud M. A. E., (2006); 'Analytical solutions of hydro magnetic boundary layer flow of a non-Newtonian power law fluid past a continuously moving surface.' Acta Mechanica Vol. 181, pp. 83 – 89.
[18] V. Marinca, N. Herisanu, (2008); 'Optimal homotopy asymptotic method with application to thin film flow.' Central European Journal of physics Vol. 6, pp. 1608 – 1644.
[19] Cheng C. Y., (2009); 'Combined heat and mass transfer in natural convection flow from a vertical wavy surface in a power-law fluid saturated porous medium with thermal and mass stratification.' International Communications in Heat and Mass Transfer, Vol. 36, pp. 351 – 356.

ISSN: 2454-1907
DOI: 10.5281/zenodo.1140081

[20] H. C. Suratiand M. G. Timol, (2010); 'Numerical Study Of Forced Convection Wedge Flow Of Some Non-Newtonian Fluids.' International Journal of Applied Mathematics and Mechanics, Vol. 6, no.18, pp. 50 – 65.
[21] Bhattacharyya K., Mukhopadhyay S., Layek G. C., (2011); 'Steady boundary layer slip flow and heat transfer over a flat porous plate embedded in a porous media.' Journal of Petroleum Science and Engineering Vol. 78, p 304.
[22] D. D. Ganji, M. Sheikholeslami, H. R. Ashorynejad, M. Zadsar & M. Esfandyaripour, (2011); 'Analytical heat transfer investigation of non-Newtonian fluid flow in an axisymmetric channel with a porous wall.' International Journal of non-linear dynamics in engineering and sciences, Vol. 3, Issue 1, pp. 103 – 110.
[23] M. B. K. Moorthy and K. Senthilvadivu, (2012); 'Effect of variable viscosity on free flow of non-Newtonian power law fluids along a vertical surface with thermal stratification.' Archives of Thermodynamics, Vol. 33, pp. 109 – 121.
[24] Shyam R, Sasmal C, Chhabra R. P., (2013); 'Natural convection heat transfer from two vertically aligned circular cylinders in power-law fluids.' International Journal of Heat and Mass Transfer Vol. 64, pp. 1127 – 1152.
[25] Hajmohammadi M. R., Nourazar S. S., (2014); 'Conjugate forced convection heat transfer from a heated flat plate of finite thickness and temperature-dependent thermal conductivity.' Heat Transfer Engineering Vol. 35, pp. 863 – 874.
[26] Sharma, R, Ishak, A., (2014); 'Second order slips flow of cu-water nano fluid over a stretching sheet with heat transfer.' WSEAS Trans. Fluid Mech, Vol. 9, pp. 26 – 33.
[27] Hayat T, Hussain M, Alsaedi A, Shehzad SA, Chen GQ (2015) Flow of power-law nanofluid over a stretching surface with Newtonian heating. Journal of Applied Fluid Mechanics 8: 273
[28] Ram Reddy, Ch, Pradeepa, T. and Srinivasacharya, D., (2015); 'Similarity Solution for Free Convection Flow of a Micropolar Fluid under Convective Boundary Condition via Lie Scaling Group Transformations.' Hindawi Publishing Corporation, Advances in High Energy Physics, Vol. 2015, Article ID 650813

*Corresponding author.
E-mail address: rky.pcm@ gmail.com